Photoemission spectra from reduced density matrices: The band gap in strongly correlated systems

Stefano Di Sabatino,[1,*] J. A. Berger,[2] Lucia Reining,[3] and Pina Romaniello[1]

[1]*Laboratoire de Physique Théorique, CNRS, IRSAMC, Université Toulouse III - Paul Sabatier, 118 Route de Narbonne, 31062 Toulouse Cedex, France, and European Theoretical Spectroscopy Facility*

[2]*Laboratoire de Chimie et Physique Quantiques, IRSAMC, Université Toulouse III - Paul Sabatier, CNRS, 118 Route de Narbonne, 31062 Toulouse Cedex, France, and European Theoretical Spectroscopy Facility*

[3]*Laboratoire des Solides Irradiés, École Polytechnique, CNRS, CEA, Université Paris-Saclay, F-91128 Palaiseau, France, and European Theoretical Spectroscopy Facility*

(Received 21 October 2015; revised manuscript received 24 September 2016; published 25 October 2016)

We present a method for the calculation of photoemission spectra in terms of reduced density matrices. We start from the spectral representation of the one-body Green's function G, whose imaginary part is related to photoemission spectra, and we introduce a frequency-dependent effective energy that accounts for all the poles of G. Simple approximations to this effective energy give accurate spectra in model systems in the weak as well as strong correlation regime. In real systems reduced density matrices can be obtained from reduced density-matrix functional theory. Here we use this approach to calculate the photoemission spectrum of bulk NiO: our method yields a qualitatively correct picture both in the antiferromagnetic and paramagnetic phases, contrary to mean-field methods, in which the paramagnet is a metal.

DOI: 10.1103/PhysRevB.94.155141

I. INTRODUCTION

Photoemission is a powerful tool to obtain insight into the electronic structure and excitations in materials. The interpretation of the experimental data is, however, a complicated task. Theory represents, hence, an essential tool for the analysis of the experiments as well as prediction of material properties. One of the most popular approaches in condensed-matter physics is many-body perturbation theory (MBPT) based on Green's functions. Within the so called GW approximation [1] to electron correlation, MBPT has become, over the last two decades, the method of choice for the calculations of quasiparticle band structures [2–7] and direct and inverse photoemission spectra [8–13] of many materials improving substantially over the results provided by static mean-field electronic structure methods. However, GW suffers from some fundamental shortcomings [14–19], and, in particular, it does not capture strong correlation, unless one treats the system in a magnetically ordered phase. In particular, many paramagnetic insulators cannot be described correctly within GW. A paradigmatic example is the case of paramagnetic NiO, which is predicted to be a metal by GW. An alternative approach based on Green's functions that can treat strongly correlated systems is dynamical mean-field theory (DMFT) [20]. However the effort to make DMFT a fully *ab initio* method is still ongoing [21]. Therefore, it is still desirable to go beyond simple approximations to the self-energy [22–29] or explore novel routes to calculate Green's functions [30,31]. In this context, promising results have been reported for model systems by expressing the one-body Green's function as a continued fraction [32] as well as for solids [33] using reduced density-matrix functional theory (RDMFT) [34]. The RDMFT framework allows for the calculation of all the ground-state expectation values as functionals of the one-body reduced density matrix (1-RDM), provided that the functional is known. This, however, is in general not the case. In particular, for spectral functions approximations have to be used.

In this work we derive an expression for the spectral function, which is related to photoemission spectra, in terms of reduced density matrices (RDMs). We show that simple approximations, which require the knowledge of the lowest n-body reduced density matrices (n-RDMs) only, can provide accurate photoemission spectra in model systems for moderate as well as for strong electron correlation. Our method overcomes the main problem of mean-field theories and GW in correlated solids: as we show with the example of NiO, it correctly predicts this material to be insulating in both the antiferromagnetic and paramagnetic phases. The paper is organized as follows. In Sec. II we derive a new expression for the spectral function in terms of RDMs, we discuss simple approximations to it, and their physical meaning. In Sec. III we illustrate, with the Hubbard model and the more realistic example of bulk NiO, how these approximations perform. Finally, in Sec. IV we draw our conclusions and perspectives.

II. THEORY

We start from the spectral representation of the time-ordered Green's function G at zero temperature, which reads

$$G_{ij}(\omega) = \sum_k \frac{B_{ij}^{k,R}}{\omega - \epsilon_k^R - \mathrm{i}\eta} + \sum_k \frac{B_{ij}^{k,A}}{\omega - \epsilon_k^A + \mathrm{i}\eta}, \qquad (1)$$

where $\epsilon_k^R = E_0 - E_k^{N-1}, \epsilon_k^A = E_k^{N+1} - E_0, B_{ij}^{k,R} = \langle\Psi_0|\hat{c}_j^\dagger|\Psi_k^{N-1}\rangle\langle\Psi_k^{N-1}|\hat{c}_i|\Psi_0\rangle, B_{ij}^{k,A} = \langle\Psi_0|\hat{c}_i|\Psi_k^{N+1}\rangle\langle\Psi_k^{N+1}|\hat{c}_j^\dagger|\Psi_0\rangle$, with E_0 and Ψ_0 the ground-state energy and wave function of the N-electron system and $E_k^{N\pm1}$ and $\Psi_k^{N\pm1}$ the kth state energy and wave function of the $(N \pm 1)$-electron system. The superscripts R and A in Eq. (1) indicate the removal and addition parts of G, respectively. In the following we concentrate on the diagonal elements of G, which are related to photoemission spectra. We choose to work in the basis set of natural orbitals ϕ_i, i.e., the orbitals that diagonalize

*disabatino@irsamc.ups-tlse.fr

the 1-RDM, $\gamma(\mathbf{x},\mathbf{x}') = \sum_i n_i \phi_i(\mathbf{x})\phi_i^*(\mathbf{x}')$, where $0 \leqslant n_i \leqslant 1$ are the occupation numbers and $\mathbf{x} = (\mathbf{r},s)$ is a combined space-spin coordinate. Note that natural orbitals with $n_i = 0$ are not uniquely defined. We fix them by assuming they correspond to the noninteracting solution. In this basis set $\sum_k B_{ii}^{k,R} = n_i$ and $\sum_k B_{ii}^{k,A} = (1-n_i)$. Inspired by the numerical effective-energy technique introduced in Refs. [35,36] that was designed to speed up convergence of a given spectral sum in the independent-particle framework, we present here a many-body effective-energy theory (MEET) to derive new expressions for the many-body spectral functions in terms of RDMs. A separate treatment of removal and addition spaces turns out to be crucial. Let us first concentrate on the removal part. We define the effective energy $\delta_i^R(\omega)$ by

$$G_{ii}^R(\omega) = \sum_k \frac{B_{ii}^{k,R}}{\omega - \epsilon_k^R} = \frac{\sum_k B_{ii}^{k,R}}{\omega - \delta_i^R(\omega)} = \frac{n_i}{\omega - \delta_i^R(\omega)}. \quad (2)$$

The effective energy $\delta_i^R(\omega)$ accounts for all the poles of the removal part of G_{ii}, which is in principle possible since it is frequency dependent. We now rewrite Eq. (2) as

$$\delta_i^R(\omega) = \frac{\tilde{G}_{ii}^R(\omega)}{G_{ii}^R(\omega)}, \quad (3)$$

where

$$\tilde{G}_{ii}^R(\omega) = \sum_k \frac{\langle\Psi_0|\hat{c}_i^\dagger|\Psi_k^{N-1}\rangle\langle\Psi_k^{N-1}|[\hat{c}_i,\hat{H}]|\Psi_0\rangle}{\omega - \epsilon_k^R}, \quad (4)$$

where $\hat{H}$ is the many-body Hamiltonian. We can now introduce another effective energy $\tilde{\delta}_i^R(\omega)$ that accounts for all the poles of $\tilde{G}_{ii}^R(\omega)$. Working out the equations one arrives at $\tilde{\delta}_i^R(\omega) = \tilde{\tilde{G}}_{ii}^R(\omega)/\tilde{G}_{ii}^R(\omega)$, with

$$\tilde{\tilde{G}}_{ii}^R(\omega) = \sum_k \frac{\langle\Psi_0|[\hat{H},\hat{c}_i^\dagger]|\Psi_k^{N-1}\rangle\langle\Psi_k^{N-1}|[\hat{c}_i,\hat{H}]|\Psi_0\rangle}{\omega - \epsilon_k^R}. \quad (5)$$

This leads to

$$\delta_i^R(\omega) = \frac{\frac{\tilde{n}_i^R}{\omega - \tilde{\delta}_i^R(\omega)}}{\frac{n_i}{\omega - \tilde{\delta}_i^R(\omega)}} = \frac{\tilde{n}_i^R}{n_i}\frac{\omega - \frac{\tilde{G}_{ii}^R(\omega)}{G_{ii}^R(\omega)}}{\omega - \frac{\tilde{\tilde{G}}_{ii}^R(\omega)}{\tilde{G}_{ii}^R(\omega)}}, \quad (6)$$

where

$$\tilde{n}_i^R = \langle\Psi_0|\hat{c}_i^\dagger[\hat{c}_i,\hat{H}]|\Psi_0\rangle. \quad (7)$$

In principle, one could continue this procedure *ad infinitum*. In practice, however, one has to truncate the series. This can be done in various ways. Here we choose a truncation that guarantees the exact results for the Hubbard dimer at 1/2 filling at all orders, as we will discuss later. This is obtained by assuming that at a certain order the poles of $G_{ii}^R, \tilde{G}_{ii}^R, \ldots$, expressed in terms of the respective effective energies $\delta_i^R, \tilde{\delta}_i^R, \ldots$, are the same. The first two approximations to $\delta_i^R(\omega)$ read

$$\delta_i^{R,(1)} = \frac{\tilde{n}_i^R}{n_i}, \quad (8)$$

$$\delta_i^{R,(2)}(\omega) = \frac{\tilde{n}_i^R}{n_i}\frac{\omega - \frac{\tilde{n}_i^R}{n_i}}{\omega - \frac{\tilde{\tilde{n}}_i^R}{\tilde{n}_i^R}}, \quad (9)$$

where $\tilde{\tilde{n}}_i^R = \langle\Psi_0|[\hat{H},\hat{c}_i^\dagger][\hat{c}_i,\hat{H}]|\Psi_0\rangle$.

Similarly for the addition energies one can introduce an effective energy $\delta_i^A(\omega)$, and derive approximations. The first two approximations to $\delta_i^A(\omega)$ read

$$\delta_i^{A,(1)} = \frac{\tilde{n}_i^A}{1-n_i}, \quad (10)$$

$$\delta_i^{A,(2)}(\omega) = \frac{\tilde{n}_i^A}{1-n_i}\frac{\omega - \frac{\tilde{n}_i^A}{1-n_i}}{\omega - \frac{\tilde{\tilde{n}}_i^A}{\tilde{n}_i^A}}, \quad (11)$$

where $\tilde{n}_i^A = \langle\Psi_0|[\hat{c}_i,\hat{H}]\hat{c}_i^\dagger|\Psi_0\rangle$, and $\tilde{\tilde{n}}_i^A = \langle\Psi_0|[\hat{c}_i,\hat{H}][\hat{H},\hat{c}_i^\dagger]|\Psi_0\rangle$. An important point to note is that for a given natural orbital ϕ_i, removal and addition effective energies are different: this is essential to open a gap, as we will illustrate in the Hubbard model.

In the following we express $\delta_i^{R/A,(n)}$, with $n = 1,2$ in terms of RDMs. Let us consider the following many-body Hamiltonian

$$\hat{H} = \hat{H}_0 + \hat{V} = \sum_i h_{ij}\hat{c}_i^\dagger\hat{c}_j + \frac{1}{2}\sum_{ijkl} V_{ijkl}\hat{c}_i^\dagger\hat{c}_j^\dagger\hat{c}_l\hat{c}_k, \quad (12)$$

where $\hat{c}_i^\dagger$ and $\hat{c}_i$ are the creation and annihilation operators in the basis of natural orbitals $\phi_i(\mathbf{x})$. Here $h_{ij} = \int d\mathbf{x}\phi_i^*(\mathbf{x})h(\mathbf{r})\phi_j(\mathbf{x})$ are the matrix elements of the one-particle noninteracting Hamiltonian $h(\mathbf{r}) = -\nabla^2/2 + v_{\text{ext}}(\mathbf{r})$, and $V_{ijkl} = \int d\mathbf{x}d\mathbf{x}'\phi_i^*(\mathbf{x})\phi_j^*(\mathbf{x}')v_c(\mathbf{r},\mathbf{r}')\phi_k(\mathbf{x})\phi_l(\mathbf{x}')$ are the matrix elements of the Coulomb interaction v_c. Using the Hamiltonian (12), we can evaluate the commutators appearing in the expressions for $\tilde{n}_i^{R/A}$ and $\tilde{\tilde{n}}_i^{R/A}$. For $\tilde{n}_i^{R/A}$ we obtain the following relations:

$$\tilde{n}_i^R = h_{ii}n_i + \sum_{jkl} V_{ijkl}\Gamma_{klji}^{(2)}, \quad (13)$$

$$\tilde{n}_i^A = h_{ii}(1-n_i) + \sum_j (V_{ijij} - V_{ijji})n_j - \sum_{jkl} V_{ijkl}\Gamma_{klji}^{(2)}, \quad (14)$$

with $\Gamma_{klji}^{(2)} = \langle\Psi_0|\hat{c}_i^\dagger\hat{c}_j^\dagger\hat{c}_l\hat{c}_k|\Psi_0\rangle$ the matrix elements of the 2-RDM. The expressions of $\tilde{\tilde{n}}_i^R$ and $\tilde{\tilde{n}}_i^A$ in terms of 1-, 2-, and 3-RDMs are given in Appendix A. Using Eqs (13), (14), (A1), and (A2) we get the expressions of $\delta_i^{R/A,(1)}$ and $\delta_i^{R/A,(2)}$ in terms of RDMs (see Appendix A).

The spectral function can then be written as

$$A_{ii}(\omega) = n_i\delta\big(\omega - \delta_i^R(\omega)\big) + (1-n_i)\delta\big(\omega - \delta_i^A(\omega)\big), \quad (15)$$

which satisfies the sum rule $\int_{-\infty}^{\infty} d\omega A_{ii}(\omega) = 1$. Starting from $\delta^{(2)}$ one could, in principle, get complex poles because the equations become nonlinear in the frequency. In this case the sum rule is not satisfied. However, such complex poles do not occur for $\delta^{(2)}$, at least in the model systems we studied. For higher-order approximations remedies such as the regularization of unphysical poles could be envisaged (see Ref. [36] for an example in the case of independent particles). Our goal here is to derive simple and physically motivated expressions for the spectral function, and this is obtained using $\delta^{(1)}$ and $\delta^{(2)}$, as we will show later.

The expression (15) looks similar to the one reported in Ref. [33] in the context of RDMFT. In that case (referred

to as DER in the following), however, removal and addition energies are calculated in a different way, namely as functional derivatives of the ground-state total energy with respect to the occupation numbers. Our method, instead, is not bound to RDMFT: it can be used with any approach that can provide one with RDMs. It does therefore not require a total energy that is a functional of occupation numbers. For example the RDMs could be obtained from quantum Monte Carlo (see, e.g., Refs. [37,38]).

The physical meaning of $\delta_i^{R,(1)}$ can be seen by combining Eqs. (7) and (8). This gives a weighted average of all removal poles of G_{ii}^R, since one gets $\delta_i^{R,(1)} = \sum_k B_{ii}^{k,R}\epsilon_k^R / \sum_k B_{ii}^{k,R}$. In other words $\delta_i^{R,(1)}$ is equal to the first moment of $G_{ii}^R(\omega)$. Here the nth moment is defined as $\mu_{n,i}^R = \sum_k B_{ii}^{k,R}(\epsilon_k^R)^n / \sum_k B_{ii}^{k,R}$. A similar relation can be derived for $\delta_i^{A,(1)}$. It is worth pointing out that $\delta_i^{R/A,(1)}$, besides reproducing the correct number of quasiparticle peaks, can also describe satellites, as we show in Sec. III. Furthermore, the first and second moments of the approximate Green's function generated by $\delta_i^{R/A,(2)}$ are equal to the first and second moments of the exact Green's function. For $\delta_i^{R/A,(n)}$ with $n > 2$ higher moments are involved [39]. Thanks to the fact that the first moment $\mu_{1,i}^R$ of the approximate Green's function is equal to the exact one, the total energy calculated using the one-body Green's function is exact, provided that the exact RDMs are used. Using the Galitskii-Migdal equation, one can indeed express the exact total energy in terms of $\mu_{1,i}^R$ and n_i as $E_0 = \sum_i n_i(\mu_{1,i}^R + h_{ii})/2$.

III. RESULTS

In this section we show how the approximations derived above work in practice.

A. Hubbard model

To test our method we apply it to the Hubbard model. The important parameters of the model are the on-site Coulomb interaction U and the hopping parameter $-t$. First, we test our method using the exact RDMs, which can be calculated for the Hubbard clusters considered here. For the Hubbard dimer at 1/2 filling the method is exact for all $\delta^{(n)}$ with $n \geqslant 1$. The case with more sites at 1/2 filling is highly nontrivial. For small rings, the simple approximation $\delta^{(1)}$ suffices to give an accurate spectrum at all interaction strengths, although it tends to overestimate the band gap. When we consider larger rings, at the level of $\delta^{(1)}$, the spectral shape is still good, but the overestimation of the band gap is more evident, as can be seen in Fig. 1 (left panel) where we present the case of a 12-site ring. Furthermore we find that, for a fixed interaction U, the ratio between the $\delta^{(1)}$ band gap and the exact band gap increases going from the one-dimensional (1D) to the two-dimensional (2D) infinite Hubbard model (see Appendix B) [40]; this suggests that the error of $\delta^{(1)}$ in reproducing the band gap increases with the dimensionality. One has to go to $\delta^{(2)}$ to partially correct this overestimation.

Also, away from 1/2 filling one has to go to $\delta^{(2)}$ to have overall better results, in particular in the atomic limit (see Fig. 2). Note that, although the spectral profile given by $\delta^{(1)}$ is in good agreement with the exact spectrum at $t = 1$, as shown

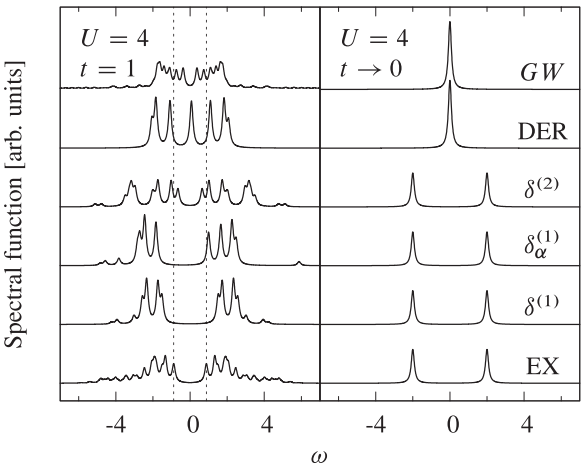

FIG. 1. Spectral function for a 12-site Hubbard ring at 1/2 filling: exact (EX) vs MEET with exact RDMs ($\delta^{(1)}$ and $\delta^{(2)}$), MEET with approximate RDMs ($\delta_\alpha^{(1)}$,$\alpha = 0.5$), DER method (with $\alpha = 0.5$), and GW method. Peaks are broadened with a Lorentzian of width $\eta = 0.1$.

in Fig. 2, the analysis of the peaks in the energy range $0 < \omega < 5$ has revealed a mixed quasiparticle/satellite character. Moreover, in the atomic limit, the main peak at $\omega = 0$ in the exact spectrum is a superposition of a removal peak and an addition peak. In this limit, $\delta^{(1)}$ opens a band gap around $\omega = 0$, which is not present in the exact results. Using $\delta^{(2)}$ tends to correct these errors. This indicates that $\delta^{(1)}$ is not a good approximation in metallic systems.

There are two striking features of the results obtained with our method: (i) there are satellites, even with a static approximation ($\delta^{(1)}$), i.e., more energies than the number of natural orbitals; (ii) there is a gap in the atomic limit (see right panel of Fig. 1) without breaking the symmetry of the system (i.e., without localizing the spins each on a site). The first feature can be understood looking at the spectral weights in the spectral function (15), which are n_i for the removal energies and $1 - n_i$ for the addition energies. As long as the occupation numbers are 0 or 1, as in the noninteracting case,

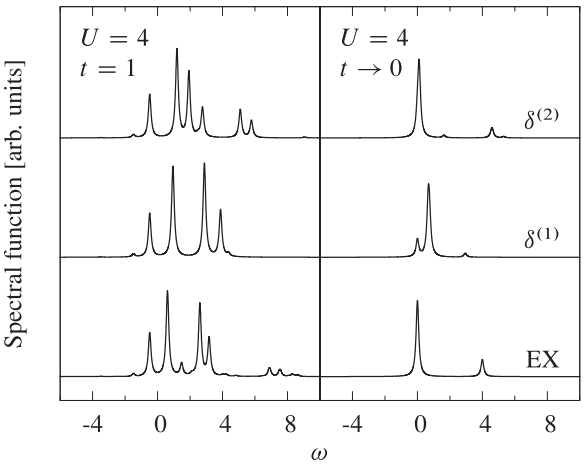

FIG. 2. Spectral function for a 6-site Hubbard ring at 1/6 filling: exact (EX) vs MEET with exact RDMs ($\delta^{(1)}$ and $\delta^{(2)}$). Peaks are broadened with a Lorentzian of width $\eta = 0.1$.

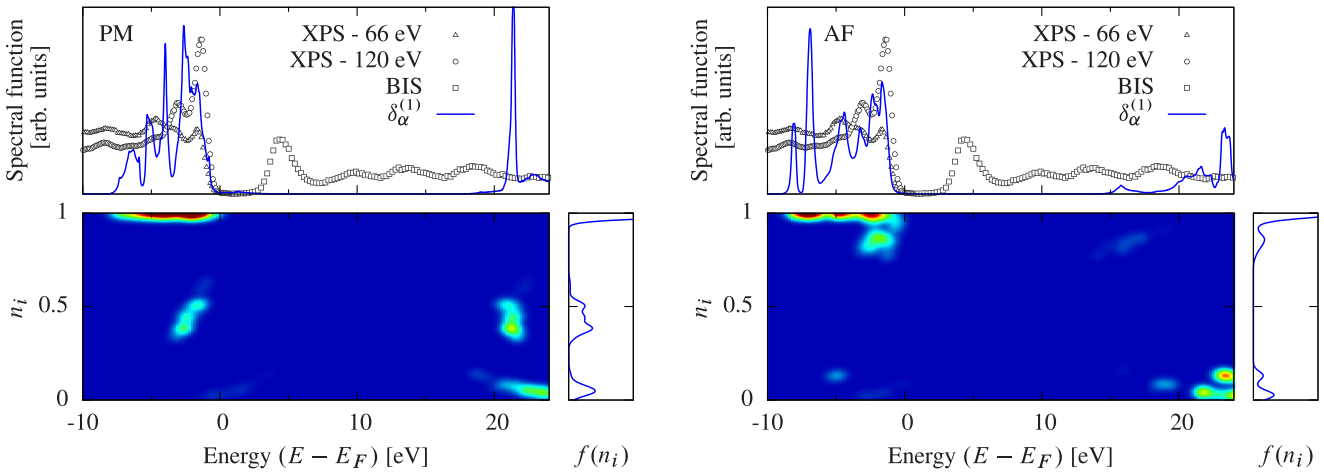

FIG. 3. Paramagnetic (left) and antiferromagnetic (right) bulk NiO: experimental photoemission spectrum [45] vs MEET spectrum ($\delta_\alpha^{(1)}$,$\alpha = 0.65$). The color map and the distribution $f(n_i)$ illustrate the occupation numbers n_i that play a role into the spectrum for the reported energy range.

for each n_i one sees either a removal or an addition peak. When, instead, $0 < n_i < 1$, then, for each n_i one gets both a removal and an addition peak. In other words, at the level of $\delta^{(1)}$, for each orbital one gets two energies. These two energies are related by:

$$\delta_i^{A,(1)} = \delta_i^{R,(1)} - \frac{1}{n_i(1-n_i)} \sum_{jkl} V_{ijkl}\Gamma^{(2)}_{c,klji}, \qquad (16)$$

where $\Gamma_c^{(2)}$ is the correlation contribution to the 2-RDM (see Appendix A). In the Hubbard dimer at 1/2 filling, for example, $\sum_{jkl} V_{ijkl}\Gamma^{(2)}_{c,klji} = -U/2\sqrt{n_b n_a}$, with n_a and n_b the occupation numbers of the bonding and antibonding natural orbitals, respectively. In the atomic limit the occupation numbers tend to 1/2, and therefore the spectral function consists of one removal and one addition energy peak of equal weight, each being a superposition of the bonding and the antibonding component; the band gap is hence between two peaks of the same component, and it equals U, as given by Eq. (16). The GW approximation, instead, can open a gap only between different components, i.e., it describes a quasiparticle gap; it hence fails to describe the correlation gap in the Hubbard dimer in the atomic limit.

Note that when the Hartree-Fock (HF) approximation is used for the 2-RDM the effective energies $\delta_i^{R/A,(1)}$ are equal to the removal/addition energies obtained with the HF self-energy. However, since $n_i = 1$ or 0, only one of the two appears in the spectral function.

In real situations the exact RDMs are not known. Here we focus on $\delta^{(1)}$, since it requires only the knowledge of the 1- and 2-RDMs, which can be obtained within RDMFT. In this framework the 2-RDM is a functional of the 1-RDM. This functional is not known, but approximations are available. In this work we will use the power functional $\Gamma^{(2)}(\mathbf{x},\mathbf{x}';\mathbf{x},\mathbf{x}') \approx \gamma(\mathbf{x},\mathbf{x})\gamma(\mathbf{x}',\mathbf{x}') - \gamma^\alpha(\mathbf{x},\mathbf{x}')\gamma^\alpha(\mathbf{x}',\mathbf{x})$ where $\gamma^\alpha(\mathbf{x},\mathbf{x}') = \sum_i n_i^\alpha \phi_i(\mathbf{x})\phi_i^*(\mathbf{x}')$, with $0.5 \leqslant \alpha \leqslant 1$ [41].

First we test this approximation on the Hubbard model. In Fig. 1 we report the results for a 12-site ring using $\alpha = 0.5$. We obtain good results (although the power functional does not recover the particle-hole symmetry) and, in particular, the band gap opens in the atomic limit without breaking the symmetry [42]. We note that the gap strongly depends on the value of α: it has its maximum value for $\alpha = 0.5$ while it disappears for $\alpha = 1$, which corresponds to HF. For comparison we also report the results obtained using GW and the DER method: in the atomic limit these methods do not open any gap, unless the symmetry of the system is broken [42]. This raises the question whether the MEET, using the simple approximations that are successful in the models, could also open the band gap of a real Mott insulator.

B. Realistic systems: the example of NiO

We implemented our approach in a modified version of the full-potential linearized augmented plane wave (FP-LAPW) code ELK [43], with practical details of the calculations following the scheme described in Ref. [41]. We apply the method to bulk NiO, which is a prototypical strongly correlated material. This system shows antiferromagnetic behavior below the Néel temperature, and the photoemission spectrum is similar for the paramagnetic and the antiferromagnetic phases [44], with a band gap of about 4.3 eV [45]. Already at the level of LSDA, the antiferromagnetic phase shows a band gap, although too small, due to quasiparticle splitting. The spectrum in this phase can be well described by GW [11,12] as well as RDMFT using the DER method [33]. However, the real challenge is to open a gap without symmetry breaking (see Appendix C) as it should happen in the paramagnetic phase. To this aim we model the paramagnetic phase as nonmagnetic. In this case the gap is purely due to correlation, which LDA and GW fail to describe. Our approach, instead, opens a gap in both phases. This is shown in Fig. 3. Note that our results for both phases are compared with experiment for the antiferromagnetic phase [45]. This comparison is meaningful since the observed photoemission spectrum of NiO is almost unaffected by the magnetic phase transition [44]. For the calculations we used the experimental lattice constants and the power functional with the self-interaction correction proposed by Goedecker and Umrigar [46]. For the power functional we

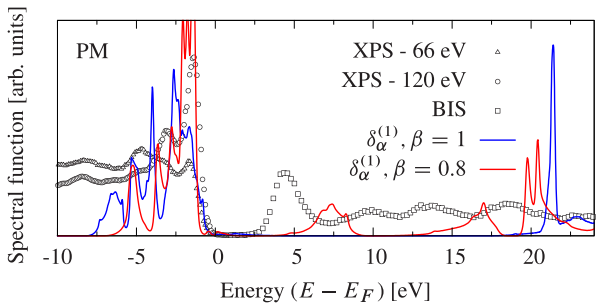

FIG. 4. Paramagnetic bulk NiO: experimental photoemission spectrum [45] vs MEET spectrum ($\delta_\alpha^{(1)}$, with the power functional, $\alpha = 0.65$, and without screening ($\beta = 1$) and with screening $\beta = 0.8$).

use the value $\alpha = 0.65$, which has been suggested in literature [41,47,48]. From the analysis of the occupation numbers it emerges that the physics underlying the band gap opening in the two phases is indeed different: in the antiferromagnetic case it is mainly due to occupation numbers close to one or zero, whereas in the paramagnetic phase it is mainly due to occupation numbers around 0.5. This is in line with an analogous analysis on the Hubbard dimer [42]. It still remains to improve the band gap, which is overestimated in our method. This finding is consistent with the results on large Hubbard rings, which indicate that this overestimation is due to the use of $\delta^{(1)}$, and that the use of $\delta^{(2)}$ might improve the spectrum and the band gap. This would require approximations for the 3-RDM, which is beyond the scope of this paper. However, we can get a rough estimation of the influence of $\delta^{(2)}$ on the spectrum of NiO by using an effective $\delta^{(1)}$ in which some of the effects due to $\delta^{(2)}$ are included. Using the 12-site Hubbard chain (for which both $\delta^{(1)}$ and $\delta^{(2)}$ can be calculated exactly) we calculated the screening of $\delta^{(1)}$ that reproduces the effect of $\delta^{(2)}$. The screening (which we call here β) depends on the component of G (i.e., on the natural orbital) one is looking at, and has been defined according to

$$\delta_i^{R,(1)} = h_{ii} + \sum_j V_{ijij} n_j + \frac{\beta_i}{n_i} \sum_{jkl} V_{ijkl} \Gamma^{(2)}_{\mathrm{xc},klji}, \qquad (17)$$

where $\Gamma^{(2)}_{\mathrm{xc},klji} = \Gamma^{(2)}_{klji} - n_i n_j \delta_{ik} \delta_{jl}$ is the exchange-correlation part of the 2-RDM (see Appendix A). For most of the natural orbitals that are responsible for the gap in the Hubbard model, the values of β_i are in the range $0 < \beta_i < 1$. Therefore, for the calculation of the spectrum of NiO, we choose β_i between 0 and 1 and assume it to be the same for each orbital. This leads to a reduction of the band gap; in particular, with $\beta = 0.8$ the spectral function of paramagnetic NiO is in better agreement with experiment, as illustrated in Fig. 4. Further decreasing β can eventually close the gap. These findings indicate that one could envisage to include in an approximate way higher-order terms using a proper terminating function. We have also applied our method to other transition-metal oxides, such as MnO, and we observe similar performances as in NiO.

IV. CONCLUSIONS AND PROSPECTIVES

In conclusion, we have derived an expression for the spectral function in terms of RDMs. Simple approximations can give accurate spectra for finite model systems in the weak as well as in the strong correlation regime. In particular the method correctly reproduces the atomic limit of Hubbard systems without breaking the symmetry of the system. We applied a simple approximation depending only on the 1- and 2-RDMs to bulk NiO within the computationally efficient RDMFT. Our method produces qualitatively correct photoemission spectra for the antiferromagnetic and paramagnetic phases, although the band gap is overestimated. The study of the Hubbard model indicates how this problem might be overcome in the future. Our method indicates a promising way to approach the problem of band gaps due to correlation effects in a relatively simple manner.

ACKNOWLEDGMENTS

The research leading to these results has received funding from the European Research Council under the European Union's Seventh Framework Programme (FP/2007-2013) / ERC Grant Agreement No. 320971. Discussion within the Collaboration Team on Correlation of the European Theoretical Spectroscopy facility (ETSF) is greatly acknowledged. S.D.S. and P.R. thank M. Gatti, M. Guzzo, and S. Sharma for fruitful discussions.

APPENDIX A: APPROXIMATIONS TO $\delta_i^{R/A}$ IN TERMS OF REDUCED DENSITY MATRICES

In the following we give the expressions of $\tilde{\tilde{n}}_i^{R/A}$ in terms of RDMs. Using the Hamiltonian (12), we can evaluate the commutators appearing in the definitions of $\tilde{\tilde{n}}_i^{R/A}$. We obtain the following relations:

$$\begin{aligned}\tilde{\tilde{n}}_i^R &= h_{ii}^2 n_i + h_{ii} \sum_{jkl} \left(V_{ijkl} \Gamma^{(2)}_{klji} + V_{jkil} \Gamma^{(2)}_{ilkj} \right) \\ &\quad + \sum_{jklk'l'} V_{jkil} V_{ilk'l'} \Gamma^{(2)}_{k'l'kj} \\ &\quad + \sum_{jklj'k'l'} V_{jkil} V_{ij'k'l'} \Gamma^{(3)}_{k'l'lj'kj}, \qquad (A1) \\ \tilde{\tilde{n}}_i^A &= h_{ii}^2 (1 - n_i) + 2 h_{ii} \sum_j (V_{ijij} - V_{ijji}) n_j \\ &\quad + h_{ii} \sum_{jkl} \left(V_{ijkl} \Gamma^{(2)}_{klij} + V_{jkil} \Gamma^{(2)}_{likj} \right) \\ &\quad + \sum_{jkl} (V_{iljk} - V_{ilkj}) V_{jkil} n_l \\ &\quad + \sum_{jklj'k'} (V_{ij'k'j} - V_{ij'jk'}) (V_{jkil} - V_{kjil}) \Gamma^{(2)}_{lk'kj'} \\ &\quad + \sum_{jklj'k'l'} V_{ij'k'l'} V_{jkil} \Gamma^{(3)}_{lk'l'kjj'}. \qquad (A2)\end{aligned}$$

where $\Gamma^{(2)}_{ijkl} = \langle \Psi_0 | \hat{c}_l^\dagger \hat{c}_k^\dagger \hat{c}_j \hat{c}_i | \Psi_0 \rangle$ and $\Gamma^{(3)}_{ijklmn} = \langle \Psi_0 | \hat{c}_n^\dagger \hat{c}_m^\dagger \hat{c}_l^\dagger \hat{c}_k \hat{c}_j \hat{c}_i | \Psi_0 \rangle$ are the matrix elements of the 2-RDM and 3-RDM, respectively.

Using Eqs (13), (14), (A1), and (A2) we get the expressions of $\delta_i^{R/A,(1)}$ and $\delta_i^{R/A,(2)}$ in terms of RDMs. Here for simplicity we give only the expressions of $\delta_i^{R/A,(1)}$; they read

$$\delta_i^{R,(1)} = h_{ii} + \frac{1}{n_i}\sum_{jkl} V_{ijkl}\Gamma^{(2)}_{klji}, \tag{A3}$$

$$\delta_i^{A,(1)} = h_{ii} + \frac{1}{1-n_i}\left[\sum_j (V_{ijij} - V_{ijji})n_j - \sum_{jkl} V_{ijkl}\Gamma^{(2)}_{klji}\right]. \tag{A4}$$

The 2-RDM can be explicitly decomposed in terms of Hartree and exchange-correlation contributions, respectively, as $\Gamma^{(2)}_{klji} = n_i n_j \delta_{ik}\delta_{jl} + \Gamma^{(2)}_{\mathrm{xc},klji}$, or in terms of Hartree, exchange, and the correlation contributions, respectively, as $\Gamma^{(2)}_{klji} = n_i n_j \delta_{ik}\delta_{jl} - n_i n_j \delta_{il}\delta_{jk} + \Gamma^{(2)}_{c,klji}$. In this case Eqs. (A3) and (A4) can be rewritten as

$$\delta_i^{R,(1)} = h_{ii} + \sum_j V_{ijij} n_j + \frac{1}{n_i}\sum_{jkl} V_{ijkl}\Gamma^{(2)}_{\mathrm{xc},klji}, \tag{A5}$$

$$= h_{ii} + \sum_j (V_{ijij} - V_{ijji})n_j + \frac{1}{n_i}\sum_{jkl} V_{ijkl}\Gamma^{(2)}_{c,klji} \tag{A6}$$

$$\delta_i^{A,(1)} = h_{ii} + \sum_j V_{ijij} n_j - \frac{1}{1-n_i}\left[\sum_j V_{ijji} n_j + \sum_{jkl} V_{ijkl}\Gamma^{(2)}_{\mathrm{xc},klji}\right] \tag{A7}$$

$$= h_{ii} + \sum_j (V_{ijij} - V_{ijji})n_j - \frac{1}{1-n_i}\sum_{jkl} V_{ijkl}\Gamma^{(2)}_{c,klji}. \tag{A8}$$

APPENDIX B: PERFORMANCE OF $\delta_\alpha^{(1)}$ IN 1D AND 2D INFINITE HUBBARD MODELS AT HALF FILLING

In Fig. 5 (top and middle panels) the fundamental gap ΔE_g, calculated using the MEET method ($\delta_\alpha^{(1)}$,$\alpha = 0.5,0.6$), is reported as a function of the interaction U for the 1D and 2D infinite Hubbard models at 1/2 filling. For the 1D system the MEET results are compared to the exact Bethe-Ansatz solution [49], whereas for the 2D system, they are compared to our exact results for finite-size 2D Hubbard clusters and the extrapolated results to the infinite 2D system. In the figure we report only the range of U for which the 2D system is an insulator. For each value of U,$\delta_\alpha^{(1)}$ can produce the correct band gap by properly tuning α.

In the bottom panel of Fig. 5 we compare the ratio between the $\delta_\alpha^{(1)}$ band gap and the exact band gap ($\Delta E_g^{\mathrm{MEET}}/\Delta E_g^{\mathrm{EX}}$) for the two Hubbard models as a function of U: for a fixed U this ratio increases with the dimensionality of the system. For large U the ratio is similar for the two systems, since in both cases the band gap tends to U.

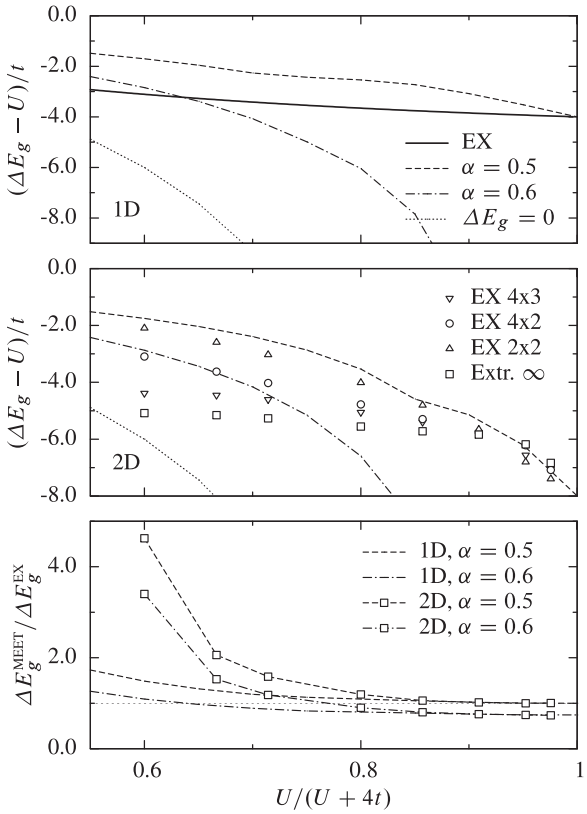

FIG. 5. Deviation of the fundamental gap ΔE_g from U as a function of $U/(U+4t)$ for the 1D (top) and 2D (middle) infinite Hubbard models at 1/2 filling. Dashed and dotted lines are obtained using the MEET method ($\delta_\alpha^{(1)}$,$\alpha = 0.5,0.6$). The black solid line in the top panel is the exact result derived from the Bethe-ansatz solution [49]. The curve corresponding to $\Delta E_g = 0$ is reported as reference. The triangles, circles, and squares in the middle panel are finite-size exact calculations for the 2×2, 4×2, and 4×3 2D Hubbard clusters, respectively. The squares are the extrapolated values to the infinite 2D system. In the bottom panel the ratio between the $\delta_\alpha^{(1)}$ band gap and exact band gap ($\Delta E_g^{\mathrm{MEET}}/\Delta E_g^{\mathrm{EX}}$) is reported as function of $U/(U+4t)$. As a guide for the eye we reported $\Delta E_g^{\mathrm{MEET}}/\Delta E_g^{\mathrm{EX}} = 1$ with a thin dashed line.

APPENDIX C: NICKEL OXIDE WITH THE DER METHOD

In Fig. 6 we report the results for NiO obtained with the DER method. In our calculations the Brillouin zone is sampled by a mesh of $6\times 6\times 6$ **k** points for the paramagnetic phase and $4\times 4\times 4$ **k** points for the antiferromagnetic phase. Both samplings include the Γ point. Moreover, we used a smearing width of 27 meV. In the antiferromagnetic phase the band gap is better reproduced than within the MEET. This can be understood by inspecting the expression for removal/addition energies in the DER method [33]. Using the power functional these energies are obtained as:

$$\epsilon_i^R = -\epsilon_i^A = \left.\frac{\partial E[\{n_k\},\{\phi_k\}]}{\partial n_i}\right|_{n_i=1/2}$$

$$= h_{ii} + \left[\sum_j V_{ijij} n_j - \alpha n_i^{\alpha-1}\sum_j V_{ijji} n_j^\alpha\right]_{n_i=1/2}. \tag{C1}$$

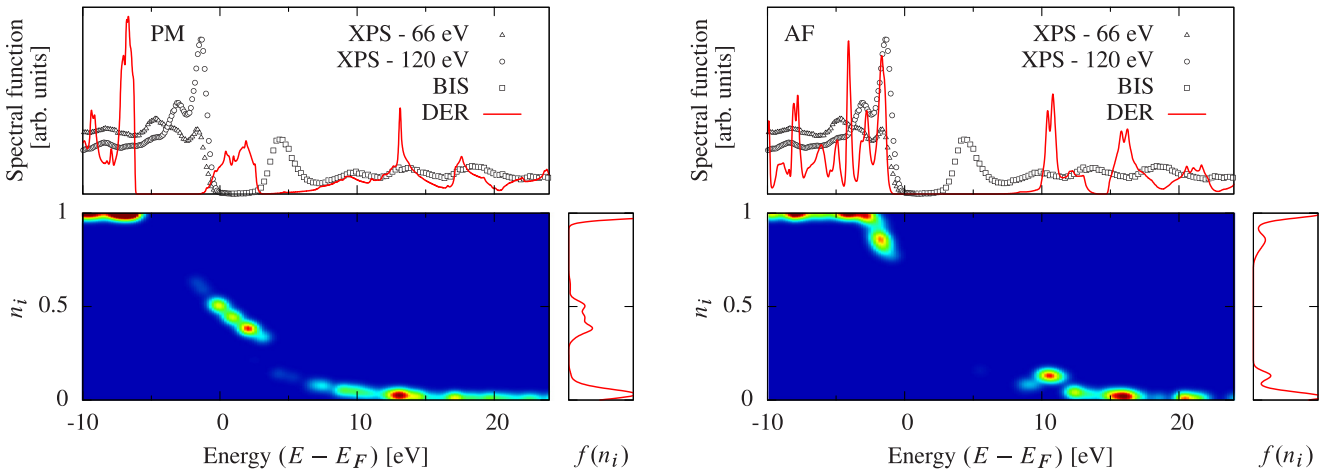

FIG. 6. Paramagnetic (left) and antiferromagnetic (right) bulk NiO: experimental photoemission spectrum [45] vs DER spectrum (with the power functional, $\alpha = 0.65$). The color map and the distribution $f(n_i)$ illustrate the occupation numbers n_i that play a role into the spectrum for the reported energy range.

This expression, which is the same for both removal and addition energies, is similar to the expression for the removal energies $\delta_i^{R,(1)}$, which, with the power functional, reads

$$\delta_i^{R,(1)} = h_{ii} + \sum_j V_{ijij} n_j - n_i^{\alpha-1} \sum_j V_{ijji} n_j^{\alpha}. \qquad \text{(C2)}$$

The difference between the two expressions resides in the prefactor α in the last term on the right-hand side of Eq. (C1), which is equal to one in Eq. (C2), and the use of $n_i = 1/2$ in Eq. (C1) instead of the value that minimizes the total energy $E[\{n_k\},\{\phi_k\}]$ [50], as in Eq. (C2). This tends to reduce the band-gap width with respect to our method. Note that with $\alpha = 1$ (HF), the two methods coincide. In the paramagnetic phase (which we model with a nonmagnetic phase), instead, we found that the DER method does not open any gap. The occupation numbers mainly involved in the band-gap region lie around 0.5 as in the MEET, however the corresponding energies accumulate in the band-gap region, whereas our method displaces them and opens a gap. Note that our DER results are different from the results reported in Ref. [51], where the DER method is shown to open a gap for a proper choice of the parameter α. However, contrary to us, the authors of Ref. [51] use a shift of the **k**-point grid. With the shift of the **k**-point grid the number of inequivalent **k** points in the irreducible Brillouin zone is higher than in the case without shift and the calculations should converge faster. However, we found that this shift opens a gap even when used with HF, which, instead, should give a metal for paramagnetic NiO [52]. Moreover, a HF calculation without shift of the **k**-point grid on a slightly deformed crystal (deformation of the order of 10^{-9} relative to the lattice constant) yields a total energy lower than the case without deformation (-1.58165×10^3 a.u. vs -1.58138×10^3 a.u.), and a gapped spectral function very similar to the one obtained with the DER method when the shift of the grid is employed. Our analysis shows that these small perturbations lead to symmetry breaking through orbital ordering, and by consequence to the opening of a quasiparticle gap. These findings suggest that the asymmetric shift of the **k**-point grid used by Sharma *et al.* [51] plays an important role in the appearance of a band gap in NiO and that there is no contradiction between our results and the ones published in Ref. [51]. It raises the question whether it is legitimate to break the orbital symmetry to model a paramagnetic system at zero temperature. This is clearly a very important issue, which deserves further investigations but is beyond the scope of this work.

In our calculations we did not use any shift of the **k**-point grid and we checked that our results are converged with respect to the number of **k** points. We have also checked whether there is a starting point dependence. However starting from LDA or LDA+U yields the same conclusions. Note that in LDA+U we do not break the spin symmetry, therefore the e_g bands are only shifted to higher energy and well separated by the t_{2g} bands, but they remain degenerate.

Of course the case of NiO is only one example, and this does not mean that the DER method does not open a gap in other paramagnetic transition metal oxides without breaking any symmetry. For example, in the case of MnO, the DER method opens a gap for certain values of α in the power functional [51]. We checked that this is the case also without a shift of the **k**-point grid.

[1] L. Hedin, Phys. Rev. **139**, A796 (1965).
[2] W. G. Aulbur, L. Jönsson, and J. W. Wilkins, Solid State Phys. **54**, 1 (2000), and references therein.
[3] F. Aryasetiawan and O. Gunnarsson, Rep. Prog. Phys. **61**, 237 (1998), and references therein.
[4] J. Vidal, S. Botti, P. Olsson, J.-F. Guillemoles, and L. Reining, Phys. Rev. Lett. **104**, 056401 (2010).
[5] J. Vidal, X. Zhang, L. Yu, J.-W. Luo, and A. Zunger, Phys. Rev. B **84**, 041109 (2011).

[6] I. A. Nechaev, R. C. Hatch, M. Bianchi, D. Guan, C. Friedrich, I. Aguilera, J. L. Mi, B. B. Iversen, S. Blügel, P. Hofmann *et al.*, Phys. Rev. B **87**, 121111 (2013).
[7] D. Waroquiers, A. Lherbier, A. Miglio, M. Stankovski, S. Poncé, M. J. T. Oliveira, M. Giantomassi, G.-M. Rignanese, and X. Gonze, Phys. Rev. B **87**, 075121 (2013).
[8] E. Papalazarou, M. Gatti, M. Marsi, V. Brouet, F. Iori, L. Reining, E. Annese, I. Vobornik, F. Offi, A. Fondacaro *et al.*, Phys. Rev. B **80**, 155115 (2009).
[9] A. N. Chantis, M. van Schilfgaarde, and T. Kotani, Phys. Rev. B **76**, 165126 (2007).
[10] M. Gatti, F. Bruneval, V. Olevano, and L. Reining, Phys. Rev. Lett. **99**, 266402 (2007).
[11] S. V. Faleev, M. van Schilfgaarde, and T. Kotani, Phys. Rev. Lett. **93**, 126406 (2004).
[12] C. Rödl, F. Fuchs, J. Furthmüller, and F. Bechstedt, Phys. Rev. B **79**, 235114 (2009).
[13] L. Y. Lim, S. Lany, Y. J. Chang, E. Rotenberg, A. Zunger, and M. F. Toney, Phys. Rev. B **86**, 235113 (2012).
[14] W. Nelson, P. Bokes, P. Rinke, and R. W. Godby, Phys. Rev. A **75**, 032505 (2007).
[15] P. Romaniello, S. Guyot, and L. Reining, J. Chem. Phys. **131**, 154111 (2009).
[16] M. van Schilfgaarde, T. Kotani, and S. Faleev, Phys. Rev. Lett. **96**, 226402 (2006).
[17] A. Stan, N. E. Dahlen, and R. van Leeuwen, J. Chem. Phys. **130**, 114105 (2009).
[18] F. Caruso, P. Rinke, X. Ren, M. Scheffler, and A. Rubio, Phys. Rev. B **86**, 081102 (2012).
[19] M. Puig von Friesen, C. Verdozzi, and C.-O. Almbladh, Phys. Rev. Lett. **103**, 176404 (2009).
[20] A. Georges, G. Kotliar, W. Krauth, and M. G. Rozenberg, Rev. Mod. Phys. **68**, 13 (1996).
[21] S. Biermann, F. Aryasetiawan, and A. Georges, Phys. Rev. Lett. **90**, 086402 (2003).
[22] M. Springer, F. Aryasetiawan, and K. Karlsson, Phys. Rev. Lett. **80**, 2389 (1998).
[23] V. P. Zhukov, E. V. Chulkov, and P. M. Echenique, Phys. Rev. Lett. **93**, 096401 (2004).
[24] P. Romaniello, F. Bechstedt, and L. Reining, Phys. Rev. B **85**, 155131 (2012).
[25] M. Guzzo, G. Lani, F. Sottile, P. Romaniello, M. Gatti, J. J. Kas, J. J. Rehr, M. G. Silly, F. Sirotti, and L. Reining, Phys. Rev. Lett. **107**, 166401 (2011).
[26] M. Guzzo, J. J. Kas, L. Sponza, C. Giorgetti, F. Sottile, D. Pierucci, M. G. Silly, F. Sirotti, J. J. Rehr, and L. Reining, Phys. Rev. B **89**, 085425 (2014).
[27] J. Lischner, D. Vigil-Fowler, and S. G. Louie, Phys. Rev. Lett. **110**, 146801 (2013).
[28] A. Grüneis, G. Kresse, Y. Hinuma, and F. Oba, Phys. Rev. Lett. **112**, 096401 (2014).
[29] J. Kuneš, V. I. Anisimov, S. L. Skornyakov, A. V. Lukoyanov, and D. Vollhardt, Phys. Rev. Lett. **99**, 156404 (2007).
[30] G. Lani, P. Romaniello, and L. Reining, New J. Phys. **14**, 013056 (2012).
[31] J. A. Berger, P. Romaniello, F. Tandetzky, B. S. Mendoza, C. Brouder, and L. Reining, New J. Phys. **16**, 113025 (2014).
[32] R. Hayn, P. Lombardo, and K. Matho, Phys. Rev. B **74**, 205124 (2006).
[33] S. Sharma, J. K. Dewhurst, S. Shallcross, and E. K. U. Gross, Phys. Rev. Lett. **110**, 116403 (2013).
[34] T. L. Gilbert, Phys. Rev. B **12**, 2111 (1975).
[35] J. A. Berger, L. Reining, and F. Sottile, Phys. Rev. B **82**, 041103(R) (2010).
[36] J. A. Berger, L. Reining, and F. Sottile, Phys. Rev. B **85**, 085126 (2012).
[37] C. Overy, G. H. Booth, N. S. Blunt, J. J. Shepherd, D. Cleland, and A. Alavi, J. Chem. Phys. **141**, 244117 (2014).
[38] G. H. Booth, A. Gruneis, G. Kresse, and A. Alavi, Nature (London) **493**, 365 (2013).
[39] We verified analytically that similar expressions are satisfied for $n > 2$, at least up to $n = 4$.
[40] Note that in the case of infinite Hubbard models we use also an approximate functional for the 2-RDM, which can also influence the band-gap results.
[41] S. Sharma, J. K. Dewhurst, N. N. Lathiotakis, and E. K. U. Gross, Phys. Rev. B **78**, 201103 (2008).
[42] S. Di Sabatino, J. A. Berger, L. Reining, and P. Romaniello, J. Chem. Phys. **143**, 024108 (2015).
[43] http://elk.sourceforge.net, 2004.
[44] O. Tjernberg, S. Söderholm, G. Chiaia, R. Girard, U. O. Karlsson, H. Nylén, and I. Lindau, Phys. Rev. B **54**, 10245 (1996).
[45] G. A. Sawatzky and J. W. Allen, Phys. Rev. Lett. **53**, 2339 (1984).
[46] S. Goedecker and C. J. Umrigar, Phys. Rev. Lett. **81**, 866 (1998).
[47] N. N Lathiotakis, S. Sharma, J. K. Dewhurst, F. G. Eich, M. A. L. Marques, and E. K. U. Gross, Phys. Rev. A **79**, 040501(R) (2009).
[48] A. Putaja and E. Räsänen, Phys. Rev. B **84**, 035104 (2011).
[49] E. H. Lieb, and F. W. Wu, Phys. Rev. Lett. **20**, 1445 (1968).
[50] Note that in practice in the ELK code only the exchange-correlation contribution is evaluated at $n_i = 1/2$.
[51] Y. Shinohara, S. Sharma, S. Shallcross, N. N. Lathiotakis, and E. K. U. Gross, J. Chem. Theory Comput. **11**, 4895 (2015).
[52] B. Szpunar, Acta Phys. Pol. A **84**, 21 (1993).